Simultaneous encoding of odors by channels with diverse sensitivity to inhibition

Elizabeth J. Hong and **Rachel I. Wilson**[*]

Department of Neurobiology, Harvard Medical School, 220 Longwood Ave, Boston, MA 02115

SUMMARY

Odorant receptors in the periphery map precisely onto olfactory glomeruli ("coding channels") in the brain. However, the odor tuning of a glomerulus is not strongly correlated with its spatial position. This raises the question of whether lateral inhibition between glomeruli is specific or nonspecific. Here we show that, in the *Drosophila* brain, focal activation of even a single glomerulus recruits GABAergic interneurons in all glomeruli. Moreover, the relative level of interneuron activity in different glomeruli is largely odor-invariant. Although interneurons are recruited nonspecifically, glomeruli differ dramatically in their sensitivity to interneuron activity, and this is explained by their varying sensitivity to GABA. Interestingly, a stimulus is typically encoded in parallel by channels having high and low sensitivity to inhibition. Because lateral inhibition confers both costs and benefits, the brain might rely preferentially on "high" and "low" channels in different behavioral contexts.

INTRODUCTION

In some brain regions, a neuron's preferred stimulus and its physical location are systematically related. In these "topographic" regions, neurons that are physically near each other often have similar tuning. Because most inhibitory interneurons act locally, inhibition in these brain regions occurs mainly between neurons whose activity is correlated (Kaas, 1997). Lateral inhibition in topographic networks allows neurons to encode finer details by removing the coarse (i.e., shared) components of their signals (Srinivasan et al., 1982). It also reduces redundancy, thereby conserving metabolic resources (Barlow, 1961). However, many brain regions are non-topographic (or only weakly topographic), where neighboring neurons can have very different stimulus preferences (Bandyopadhyay et al., 2010; Ohki et al., 2005; Redish et al., 2001; Rothschild et al., 2010; Soucy et al., 2009; Stettler and Axel, 2009). In general, it is not clear to what extent lateral inhibitory connections are selective in non-topographic networks.

An example of a non-topographic circuit is the brain's first odor processing relay, the antennal lobe in insects and the olfactory bulb in vertebrates (Vosshall and Stocker, 2007;

Shepherd and Greer, 1998). Each processing channel (or "glomerulus") in this circuit receives convergent projections from many olfactory receptor neurons (ORNs), all of which express the same odorant receptor. Within each glomerulus, ORNs synapse onto second-order neurons, each of which receives direct ORN input from just one glomerulus. Thus, each glomerulus defines a discrete processing channel. Although each glomerulus has a stereotyped location, the arrangement of glomeruli displays little or no topography – i.e., odor-evoked input to glomeruli that are physically near one another is no more correlated than the input to any random pair of glomeruli (Couto et al., 2005; Hallem and Carlson, 2006; Soucy et al., 2009).

Odors typically activate multiple ORN types, and the output of a glomerulus depends on its interactions with other co-activated glomeruli. In particular, glomeruli inhibit each other via inhibitory local interneurons ("lateral inhibition"). One fact relevant to lateral inhibition is that odor-evoked activity tends to be correlated across ORNs, meaning that an odor that strongly activates one ORN type typically elicits strong activity in many other ORN types (Haddad et al., 2010; Olsen et al., 2010; Luo et al., 2010). One proposed function of lateral inhibition is to reduce these correlations at the level of second-order neurons (Cleland, 2014; Wilson, 2013).

An important outstanding question in olfaction is the degree of selectivity in lateral inhibition. In the olfactory bulb, the evidence for selective connectivity is mixed (Fantana et al., 2008; Luo and Katz, 2001; Willhite et al., 2006). Physiological studies in the olfactory bulb have inferred lateral inhibitory connectivity indirectly, based on the premise that anti-correlated activity in two glomeruli reflects an inhibitory connection between them. This question can be addressed more directly in the *Drosophila* antennal lobe. The *Drosophila* antennal lobe is compact and genetically accessible, and the activity of inhibitory local neurons (LNs) can be optically monitored within each glomerulus (Ng et al., 2002; Silbering et al., 2008). Lateral inhibition in this circuit is known to play a key role in gain control (Olsen and Wilson, 2008; Root et al., 2008) and may have other functions as well.

Here we address two outstanding questions regarding interglomerular inhibition. First, how specific are inhibitory interactions between glomeruli? Previous studies have suggested that inhibition is sparse and specific (Girardin et al., 2013; Ng et al., 2002), or pan-glomerular (Asahina et al., 2009; Olsen et al., 2010), or both (Sachse and Galizia, 2002; Silbering and Galizia, 2007; Silbering et al., 2008). Some individual LNs innervate all glomeruli, whereas others innervate just a subset of glomeruli, so any of these scenarios are possible (Chou et al., 2010; Seki et al., 2010; Okada et al., 2009).

Second, are all glomeruli equally sensitive to the effects of LN activation? Glomeruli are differentially innervated by individual inhibitory local neurons (Chou et al., 2010). Glomeruli also express variable levels of GABA receptor and show variable responses to a synthetic $GABA_B$ agonist (Root et al., 2008). In principle, either mechanism could produce variations in sensitivity to LN activation, but this has not been investigated.

In this study, we find that the recruitment of inhibition is relatively nonspecific, and indeed, activating a single glomerulus recruits LN activity in all glomeruli. Nonetheless, glomeruli

vary dramatically in their sensitivity LN activation – i.e., their "inhibitability". We propose that this organization allows some channels to realize the benefits of lateral inhibition, while allowing other channels to remain relatively immune from the costs of lateral inhibition — namely, noise and ambiguity. These results have broad relevance for how population diversity within a circuit can resolve competing constraints on neural processing.

RESULTS

Input to a single glomerulus recruits local neuron activity in all glomeruli

We began by asking whether inhibitory interactions between glomeruli are specific. We selected odor stimuli that excite only one ORN type, and we asked how the spatial pattern of activity in GABAergic local neurons (LNs) depends on the identity of the glomerulus that is receiving direct ORN input. If inhibition is sparse and glomerulus-specific, the glomerular pattern of LN activity should be different for odors that activate different ORN types, and focal stimulation should in principle be the clearest way to reveal this.

We identified eight odor stimuli that should drive activity primarily in a single ORN type, which we call "private" odor stimuli (Hallem and Carlson, 2006; Olsen et al., 2010; Schlief and Wilson, 2007). To visualize the pattern of ORN input evoked by each stimulus, we expressed the genetically encoded calcium indicator GCaMP3 (Tian et al., 2009) in ORNs under the control of the Gal4-UAS system. We then used *in vivo* two-photon microscopy to image odor-evoked signals in ORN axons terminating in the antennal lobe. As expected, each private odor stimulus elicited a fluorescence increase at the position corresponding to its cognate glomerulus (Figure 1A, B). In some experiments, one or two additional glomeruli were also weakly activated, but this was unusual.

To visualize LN activity elicited by focal ORN input, we expressed GCaMP3 in a large subset of GABAergic LNs using the *NP3056-Gal4* driver (Chou et al., 2010) and imaged calcium signals in LN neurites. The *NP3056-Gal4* driver labels between 50 – 60 LNs in the antennal lobe, and most individual LNs in this population innervate most or all glomeruli (Chou et al., 2010), which is typical of GABAergic LNs in general (Chou et al., 2010; Seki et al., 2010; Okada et al., 2009). Thus, the calcium signal in each glomerulus represents the pooled activity of many LNs, and the signal in every glomerulus originates from mostly the same group of individual LNs.

We found that each private odor elicited LN activity in all glomeruli (Figure 1C, D, and data not shown). Moreover, similar spatial patterns of activity were elicited by different odors. This outcome was observed in two independent rounds of experiments performed with different odor stimulus sets, each containing four private odors (odor set 1 and odor set 2). Similar results were also observed with a second Gal4 driver that labels about 25 – 30 GABAergic LNs (*GH298-Gal4*; Figure S1). These two LN drivers are expressed in large but mostly non-overlapping subsets of LNs. Together, they cover 8 of the 9 major morphological types of GABAergic LNs, including both pan-glomerular LNs and LNs with selective glomerular innervation patterns (Chou et al., 2010). Both drivers and all odors produced essentially the same global pattern of LN activity.

To evaluate the similarity across brains in the spatial pattern of LN activity, we computed the average response across odors for each brain, and measured the relative level of LN calcium signal in different glomeruli in that average image (Figure 1E). This quantification showed that the relative level of LN activity varied about three-fold across glomeruli, with each glomerulus exhibiting a characteristic level of activity in every brain. The differences between glomeruli in the average amount of odor-evoked LN calcium signal may reflect spatial heterogeneities in calcium entry, buffering, or extrusion across the branches of individual LNs.

Although the spatial patterns of LN activity were relatively stimulus-invariant, small differences were observed for some stimuli (Figure 1C,D). To search for putative odor-specific patterns of LN activity in an unbiased manner, we used principal component analysis (PCA). In each imaging plane, we performed PCA on the four images that were collected in the same experiment, one image for each odor. If all odors elicited the same pattern of activity, then almost all of the variance across odors would be explained by one "basis image" (i.e., the first principal component or PC1) that resembles the average across odors, and the remaining basis images (PC2 and upward) would simply capture noise. This prediction was largely true: PC1 captured the stereotyped and global spatial pattern evoked by all odors (Figure 2A,B), and it accounted for most of the explainable variance in the data (Figure S2). However, PCA also pulled out three glomeruli that were modulated independently of other glomeruli. These three glomeruli are DA2, VL2a, and V. These are the cognate glomeruli for geosmin, phenylacetaldehyde, and CO_2, respectively, and they each consistently emerged as PC2 in the appropriate position and imaging plane in the experiments that included these odors (odor set 2, Figure 2B).

Thus, although all stimuli elicited a similar overall spatial pattern of LN activity, some private odor stimuli appeared to elicit additional activity in their cognate glomerulus. To test this idea directly, we quantified the amount of LN activity in each of the eight glomeruli targeted by our "private" odors. As expected, we found that LN activity in DA2, VL2a, and V was significantly stronger when the stimulus was the cognate private odor for that glomerulus, as compared to other odors (Figure 2C). For all other glomeruli (DM4, VM7, VA6, DL1, and DL5), there was no significant difference between the level of LN activity elicited by their cognate private odor and other odors (Figure 2C). This analysis confirms the results of the unbiased PCA search: some stimuli elicit additional intraglomerular inhibition, as well as recruiting lateral inhibition to all other glomeruli.

In addition, these results indicate that PCA can successfully identify glomeruli that are recruited in an odor-specific manner. Notably, no other individual glomeruli, or subsets of glomeruli, were observed in any principal components. Thus, although PCA is demonstrably able to identify single glomeruli that are modulated in an odor-specific manner, it does not identify any additional glomeruli where LN activity is co-modulated. This analysis argues that there are no strong inhibitory subnetworks linking specific groups of glomeruli.

Next, we asked whether these results generalize across a range of odor concentrations. We tested a family of concentrations for several odors. In each case, we found that the relative level of LN activity in different glomeruli was similar across odor concentrations. However,

the overall level of LN activity grew with increasing concentration (Figure 3A,C). Higher concentrations activate more ORN types, and also drive higher spike rates in activated ORNs (Hallem and Carlson, 2006). Both mechanisms are likely to contribute to the overall increase in LN activity.

When we averaged LN activity across the antennal lobe and plotted this against the logarithm of the odor-evoked field potential recorded from ORNs (Figure 3B), we observed a linear relationship for all odors (Figure 3D). Because the ORN field potential scales linearly with the total number of ORN spikes (Olsen et al., 2010), we can infer that LN activity scales with the logarithm of total ORN spike rate.

Interestingly, not all odors were equally efficient at recruiting LN activity, even when they evoked equal levels of total ORN activity. For example, 10^{-4} pentyl acetate and 10^{-6} E2-hexenal elicited similar levels of total ORN activity (Figure 3B). However, 10^{-4} pentyl acetate elicited stronger overall LN activity than did 10^{-6} E2-hexenal (Figure 3A, C–E). This difference may reflect the fact that the pentyl acetate stimulus elicits ORN spiking that is distributed across more ORN types (Hallem and Carlson, 2006). Alternatively, or in addition, some ORN or PN types may make particularly strong synapses onto LNs.

In sum, these results show that ORN input to a single glomerulus can recruit LN activity globally in all glomeruli, and that the relative level of LN activity across most glomeruli is similar for all odor stimuli. Stimulation of some ORN types elicits additional LN activity in their target glomeruli. Finally, the level of LN activity in each glomerulus scales with the logarithm of total ORN firing rate. Taken together, these results indicate that lateral inhibition in the antennal lobe is broadly recruited by inputs pooled across most glomeruli, and argue against selective interactions between neurons corresponding to specific subnetworks of glomeruli.

Lateral inhibition is target-specific

We next turned our attention from the recruitment of LNs, to the consequences of LN activation. In particular, we asked whether LN activation has different effects on different antennal lobe projection neurons (PNs), the second-order neurons of the olfactory system. To activate LNs, we used an optogenetic method rather than odor stimuli, an approach which confers several advantages. First, by not using odors, we avoided eliciting varying levels of excitation to different PNs, a situation that would confound our measurements of inhibition in PNs. Second, optogenetics allows for the direct, robust, and scalable activation of LNs.

We expressed the light-activated cation channel channelrhodopsin-2 (ChR2) in a large subset of LNs, under the control of *NP3056-Gal4*. Whole-cell recordings from LNs that express ChR2 confirmed that LN spike rates rise with increasing light intensity, and light evokes no response in ChR2-negative LNs (Figure S3). Calcium imaging of ChR2-mediated LN activation revealed that interleaved light and odor stimuli elicit essentially identical spatial patterns of LN activity (Figure 4A, B). Thus, optogenetic LN activation serves as a convenient stand-in for odor-evoked LN activation.

To measure the consequences of LN activation, we monitored spontaneous excitatory postsynaptic currents (sEPSCs) in PNs, which arise from spontaneous spiking in ORNs (Figure 4C; Kazama and Wilson, 2008, 2009). Spontaneous EPSCs are a sensitive measure of inhibition because the primary locus of GABAergic inhibition is at ORN axon terminals, with a more minor role for inhibition at PN dendrites (Olsen and Wilson, 2008; Root et al., 2008). We note that stimulating GABAergic LNs can recruit not only lateral inhibition, but also lateral excitation, because GABAergic LNs are electrically coupled to specialized cells that also couple to PNs (Huang et al., 2010; Yaksi and Wilson, 2010). To eliminate this confound, we conducted these experiments in a genetic background that blocks these electrical connections (shakB mutant; Yaksi and Wilson, 2010).

We observed that optogenetic activation of LNs suppressed sEPSCs in most PNs, and this effect was blocked by GABAreceptor antagonists (Figure 4C, D). In PNs, increasing light intensity increased the suppression of sEPSCs (Figure 4E), and we took the slope of the relationship between sEPSC activity and light intensity as a measure of the sensitivity of each PN to LN activation (Figure 4F). As a control, we confirmed there was little effect of light in control genotypes (Figure 4E, F).

We then measured sensitivity to inhibition in a large PN cohort. Each PN was filled with biocytin and was visualized after the recording to identify the glomerulus containing its dendrites (Figure 5A). We recorded from a large number of PNs (n=46) such that many glomeruli were sampled multiple times. We normalized each PN's sensitivity to that of the most sensitive PN, so that the most sensitive PN is assigned a value of 1. Strikingly, we observed that sEPSCs were completely suppressed in the most sensitive PNs, whereas sEPSCs were almost completely unaffected in other PNs (Figure 5B). Across the population of PNs we sampled, sensitivity to LN activation was continuously and roughly normally distributed (Figure 5C). Finally, PNs corresponding to the same glomerulus were significantly more similar than PNs belonging to different glomeruli (Figure 5D). Together, these results indicate that glomeruli vary significantly in their sensitivity to GABAergic inhibition, and that sensitivity to inhibition is a stereotyped property of each glomerulus, ranging from near-total insensitivity to near-total inhibition. In other words, inhibition is "target specific", even though interneurons are recruited nonspecifically.

Variation in GABA release does not explain why glomeruli vary in their sensitivity to inhibition

What mechanisms explain why some glomeruli are very sensitive to LN activation, while others are very insensitive? One obvious possible mechanism is the variation across glomeruli in LN calcium signals (Figure 1E), which would lead to differences in GABA release. However, variation in LN calcium correlated only weakly with variation in sensitivity to LN activation, and this correlation fell short of statistical significance (Figure 6A). Variation in LN calcium may indeed be a mechanism that generates functional diversity across glomeruli, but it is evidently not the major mechanism. It appears to be overshadowed by a larger source of functional diversity.

GABA release may also be affected by variation in LN innervation density (Chou et al., 2010; Das et al., 2008; Okada et al., 2009; Seki et al., 2010; Wilson and Laurent, 2005).

Note that variation in LN innervation density does not necessarily produce variation in LN calcium signals, because LN calcium signals are normalized to resting fluorescence (F/F); thus, these are potentially independent sources of functional diversity. To measure LN innervation density, we expressed a marker of neurotransmitter release sites (bruchpilot:GFP) in a large group of LNs (Figure 6B). Confocal imaging showed that the density of LN release sites varied about two-fold across glomeruli, and these levels were stereotyped across brains, with each glomerulus exhibiting a characteristic density (Figure 6B). However, variation in the density of LN release sites was not correlated with sensitivity to LN activation (Figure 6C). Moreover, the density of LN release sites varied over a substantially smaller range than did sensitivity to inhibition. We also obtained similar results with two additional anatomical markers (n-synaptobrevin:GFP and CD8:GFP) (Figure S4). Additionally, we note that variation across glomeruli in LN innervation density was also not correlated with variation in odor-evoked LN calcium signals ($R^2 = 0.004$, p = 0.77, Figure S4), implying that these two determinants of GABA release do not reinforce each other.

In sum, there are mechanisms that may cause GABA release to vary across glomeruli: LN calcium increases are nonuniform, and LN innervation density is nonuniform. However, these two mechanisms are not correlated with each other. Nor are they significantly correlated with variations in the overall magnitude of inhibition in response to LN activation. This motivated us to investigate a postsynaptic mechanism instead.

Sensitivity to GABA varies across glomeruli

Variation in sensitivity to GABA is another mechanism that could explain the variation in sensitivity to LN activation. To investigate this idea, we used full-field photolysis of DPNI-caged GABA (Trigo et al., 2009) to deliver a brief pulse of GABA to the brain. This approach is more reproducible than iontophoresis or pressure ejection, and, because neurotransmitter is delivered rapidly, this method avoids GABA receptor desensitization.

In most PNs, GABA robustly suppressed sEPSCs, and this effect was reversibly blocked by GABA receptor antagonists (Figures 7A, B). Increasing light intensity increased the suppression of sEPSCs (Figure 7C). The slope of the relationship between sEPSC activity and light intensity was taken as the measure of GABA sensitivity of each cell (Figure 7D). As a control, we confirmed that the flash of uncaging light had little effect on sEPSC activity in the absence of caged GABA, even at the highest intensities (Figure 7D).

We measured GABA sensitivity in a large PN cohort, again using biocytin fills to identify the glomerulus containing the dendrites of each PN. In the course of many recordings, a large number of glomeruli were sampled multiple times each. For several of the sampled glomeruli, we subsequently identified Gal4-drivers that label their corresponding PNs, enabling us to make targeted recordings of GFP-labeled PNs to increase the number of replicates for those glomeruli. In total, we recorded from 52 cells.

GABA sensitivity varied dramatically across glomeruli, from essentially zero suppression to complete suppression (Figure 8A). Across the entire population, GABA sensitivity was continuously and roughly normally distributed (Figure 8B). PNs corresponding to the same glomerulus had much more similar sensitivities to GABA than PNs from different glomeruli

(Figure 8C), indicating that sensitivity to GABA is a highly stereotyped feature of each glomerulus.

We found that sensitivity to LN activation, measured by optogenetic activation of LNs (Figure 5), was highly correlated with sensitivity to GABA (Figure 8D). For instance, PNs corresponding to glomerulus DC4 were among the least sensitive to both GABA and LN activity, whereas PNs corresponding to VA3 were among the most sensitive to both GABA and LN activity. Strikingly, sensitivity to LN activation and sensitivity to GABA both vary over a wide range across glomeruli (Figure 8E), consistent with the idea that variation in GABA sensitivity is large enough to account for the variation in sensitivity to inhibition.

Overall, our results support a model where sensitivity to LN activation is primarily specified by sensitivity to GABA. In other words, the lifetime strength of lateral inhibition in each glomerulus is mainly an autonomous feature of that glomerulus, not a property of the LN network. Although the properties of the LN network do vary across glomeruli – namely, calcium signals and innervation density – these variations are relatively modest, and are not strongly correlated with sensitivity to inhibition.

Sensitivity to inhibition is independent of odor tuning

Glomeruli with high and low sensitivity to inhibition are spatially distributed throughout the antennal lobe (Figure 9A). What is the relationship between the strength of inhibition in a glomerulus and its odor tuning? We took advantage of a large data set of the odor response profiles of *Drosophila* odorant receptors (Hallem and Carlson, 2006). Each receptor in that data set can be matched with a glomerulus (Couto et al., 2005; Fishilevich and Vosshall, 2005). For each glomerulus present in both that data set and ours, we asked whether there is a systematic relationship between tuning breadth and sensitivity to LN activation, or sensitivity to GABA. We quantified tuning breadth using the lifetime sparseness metric, which describes narrowness of tuning over all stimuli (Vinje and Gallant, 2000).

Notably, tuning breadth was uncorrelated with either sensitivity to LN activation or sensitivity to GABA (Figure 9B, C). Similar results were obtained using other measures of tuning breadth, including the total lifetime activation of the odorant receptor across all odors, and the percentage of odors that elicit inhibitory responses in that odorant receptor (R^2 values range from 0.02 to 0.23, and p-values range from 0.23 to 0.72, across all comparisons). Thus, sensitivity to inhibition is independent of tuning breadth. This result is clearly illustrated by four glomeruli that are particularly narrowly tuned: DA1, VA1d, and VA1v, which respond selectively to fly pheromones; and DA2, which responds selectively to an aversive odor produced by microbes (Stensmyr et al., 2012; van der Goes van Naters and Carlson, 2007; Clyne et al., 1997). Although these glomeruli are all extremely narrowly tuned, their sensitivities to LN activation (and/or GABA) bracket the entire observed distribution (Figure 9B, C).

Next, we asked if glomeruli that prefer the same odors have more similar sensitivities to inhibition. For each pairwise combination of glomeruli, we computed the Euclidean distance between their odor response profiles, and also the difference in their sensitivity to LN activation. As before, these measurements were uncorrelated (Figure 9D). An analysis of

differences in sensitivity to GABA yielded similar results (Figure 9E). Finally, neither sensitivity to LN activation nor sensitivity to GABA correlates with the position of each glomerulus in odor response space, as described by PCA (R^2 ranges from 10^{-6} to 0.053, p-values range from 0.55 to 0.99, for loadings on PC1 – PC3). Together, these analyses imply that susceptibility to inhibition is independent of odor tuning.

As a consequence of this organization, a single odor can elicit activity in multiple glomeruli having very different sensitivities to inhibition. For example, glomeruli DL2 and DC4 are robustly co-activated by several organic acids, including propionic acid and butyric acid (Ai et al., 2010; Silbering et al., 2011; Yao et al., 2005), but these are among the most sensitive and least sensitive glomeruli to inhibition. Several alcohols and esters (Hallem and Carlson, 2006) co-activate glomeruli DM5, DM6, VM5v, and VC4, but whereas the first two glomeruli in this list are relatively sensitive to inhibition and/or GABA, the other two are relatively insensitive.

These findings indicate that heterogeneity in sensitivity to inhibition represents an axis of glomerular specialization which is orthogonal to odor tuning. Thus, most odors are likely to activate an ensemble of glomeruli having varied sensitivities to inhibition. As a result, an odor will be encoded in parallel by channels which are subject to relatively strong lateral inhibition, and channels which are only weakly affected by lateral inhibition.

DISCUSSION

Odor-invariant recruitment of global lateral inhibition

In topographic circuits, lateral inhibition occurs preferentially between neurons having similar stimulus tuning (Kaas, 1997). This organization means that inhibition would be recruited most powerfully when it is predicted to be most useful for implementing gain control and reducing correlations – i.e., when this population of neurons is collectively receiving strong excitatory input.

Here we describe an extreme example of a different circuit organization. We find that stimulating even a single glomerulus recruits GABAergic inhibition in all glomeruli. Inhibition scales with the log intensity of input to the circuit, and is almost completely untuned to odor identity (i.e. the identity of the glomerulus whose cognate ORNs are active). Thus, the signals that recruit lateral inhibition are pooled broadly across most or all channels in the circuit. This architecture finds parallels in several non-topographic or only weakly topographic regions of vertebrate neocortex where inhibition is also poorly tuned (Liu et al., 2011; Poo and Isaacson, 2009; Wu et al., 2008). Untuned inhibition in these non-topographic regions likely reflects the unbiased local pooling of diverse excitatory inputs from nearby neurons onto individual inhibitory interneurons (Bock et al., 2011). Thus, the antennal lobe can be viewed as a microcircuit which implements inhibition via unbiased pooling; this microcircuit organization may be repeated on a local scale in more complex vertebrate circuits.

Notably, a few odors elicited additional LN activity in the glomerulus directly targeted by the ORNs they activated. Intriguingly, these odors (geosmin, phenylacetaldehyde, and CO_2)

convey signals of particular behavioral relevance to the fly, and they are unusually selective for a single ORN type over a wide concentration range (Stensmyr et al., 2012; Grosjean et al., 2011; Suh et al., 2004; de Bruyne et al., 2001). Thus, when an odor activates these ORNs, the rest of the ORN population is typically quiet. Gain control in these glomeruli must therefore rely more heavily on intraglomerular inhibition, rather than lateral inhibition. For this reason, it may be useful to have unusually strong intraglomerular inhibition in these glomeruli. By contrast, a typical glomerulus receives ORN input which is correlated with ORN input to many other glomeruli (Haddad et al., 2010; Olsen et al., 2010; Luo et al., 2010). Gain control in a typical glomerulus can therefore rely on both lateral inhibition and intraglomerular inhibition.

As a population, GABAergic LNs ramify throughout the antennal lobe, making connections with all glomeruli. Most individual LNs also ramify throughout most or all glomeruli (Chou et al., 2010; Seki et al., 2010; Okada et al., 2009). However, anatomy alone cannot tell us whether inhibition is recruited in a stimulus-specific manner. One reason is that some LNs arborize in small subsets of glomeruli (Chou et al., 2010; Seki et al., 2010; Okada et al., 2009) and in principle these LNs might mediate inhibitory subnetworks between specific glomeruli. Selective subnetworks might also arise within panglomerular LNs due to passive electrotonic compartmentalization (Christensen et al., 2001) or active conductances that could shape the path of voltage propagation within an LN (Husch et al., 2009). However, our results indicate that such subnetworks do not contribute measurably to the spatial pattern of overall GABAergic inhibition in the *Drosophila* antennal lobe.

Functional implications of broad lateral inhibition

Lateral inhibition in this circuit increases the selectivity of PN responses to odors (Olsen and Wilson, 2008; Olsen et al., 2010). At first blush, this seems incompatible with our finding that inhibition is global and untuned. How can untuned inhibition narrow tuning?

Untuned inhibition can narrow tuning if it interacts with a nonlinearity. If the nonlinearity is postsynaptic – namely, the spike threshold – the result is the so-called "iceberg effect": the iceberg of synaptic drive is pushed down by inhibition, and so its profile becomes narrower (Isaacson and Scanziani, 2011; Vidyasagar et al., 1996). In the olfactory circuit we describe here, the mechanism is likely to be different, because lateral inhibition acts primarily on the presynaptic side of the ORN-to-PN synapse, with only a minor postsynaptic component (Olsen and Wilson, 2008; Root et al., 2008). Like virtually all synapses, this synapse is nonlinear, because vesicular release saturates at high presynaptic firing rates (Kazama and Wilson, 2008). A simple model predicts that this saturation broadens the tuning of the postsynaptic cell (Abbott et al., 1997). Presynaptic lateral inhibition decreases the probability of vesicular release (Olsen and Wilson, 2008), which should counteract saturation and re-narrow the postsynaptic tuning curve.

Importantly, this effect is dynamic, because our results demonstrate that LN activity grows with ORN input to the entire circuit. Provided that lateral inhibition grows as input to the circuit increases, theoretical models show that even all-to-all inhibition can reduce redundancy in neural codes, improve stimulus separability, and confer robustness to stimulus intensity (Cleland et al., 2007; Luo et al., 2010; Olsen et al., 2010).

What might be the benefit of recruiting inhibition in each glomerulus on the basis of activity in all glomeruli – rather than just a subset of glomeruli? One potential benefit would be to minimize noise. A major function of inhibition in this circuit is gain control – i.e., a negative feedback loop that keeps circuit output within a relatively narrow dynamic range. When the signal that drives gain control is noisy, then gain control will re-inject that noise into a circuit (Rieke and Rudd, 2009). This effect is most pronounced when the signals that drive gain control are pooled over a small region, in either time or space (Dunn and Rieke, 2008). PN activity is noisy, and most of this noise comes from ORNs (Kazama and Wilson, 2009; Bhandawat et al., 2007). Because noise in different ORNs is independent (Kazama and Wilson, 2009), pooling signals over many glomeruli may provide an avenue for LNs to reduce the noise that they re-inject into the circuit.

Target specificity of lateral inhibition

A major finding of our study is that, whereas recruitment of LNs is independent of cell identity, glomeruli vary widely in their sensitivity to lateral inhibition. Activity in some glomeruli was nearly completely suppressed by optogenetic activation of LNs, whereas activity in other glomeruli was almost completely unaffected. Sensitivity to inhibition was a stereotyped property of each glomerulus, with the same glomerulus having a similar level of sensitivity in different brains.

In other neural circuits, there are many examples of target neurons receiving inhibition selectively from specific classes of inhibitory neurons (e.g., Briggman et al., 2011; Gibson et al., 1999; Yoshimura and Callaway, 2005). Our study illustrates a different type of specificity. Namely, our study represents one of the clearest demonstrations of systematic differences across target neurons in the overall strength of inhibition, pooled across all inhibitory inputs to a target neuron and across all stimuli.

Our results show that the major mechanism underlying heterogeneous sensitivity to inhibition is variation in GABA sensitivity. GABA sensitivity was highly correlated with sensitivity to LN activation on a glomerulus-by-glomerulus basis. In contrast, we found no significant correlation between sensitivity to LN activation and the factors affecting GABA release (i.e., LN calcium signals and the density of LN release sites). Taken together, these results support the idea that variations in the overall level of inhibition across glomeruli are primarily specified by variations in target sensitivity to GABA, with a more minor role for variations in GABA release.

Functional implications of target specificity

What might be the function of glomeruli that are relatively insensitive to LN activation? These glomeruli might be particularly useful when it is important to minimize noise. LNs are clearly a source of noise: they spike intermittently even in the absence of a stimulus, and their odor responses vary from trial to trial (Wilson and Laurent, 2005; Chou et al., 2010). This is true even though LNs can reduce their noise by pooling excitation from many glomeruli. Noise arising from LNs is visible in recordings from PNs (Kazama and Wilson, 2009). Glomeruli that are insensitive to inhibition would be immune to this noise. We

propose that higher brain areas might rely on these glomeruli when the odor signals are weak and near the noise threshold for detection.

Glomeruli that are insensitive to inhibition are also potentially useful encoders of absolute odor concentration. Absolute odor concentration must be encoded in the activity of some PNs, because flies can remember the concentration of an odor they were trained to avoid (Dudai, 1977; Yarali et al., 2009). This is not a trivial problem: as we show, LN activity grows with odor concentration, and so increases in inhibition counter increases in stimulus intensity, potentially creating ambiguity about odor concentration in higher brain regions. Glomeruli that are insensitive to inhibition should have the steepest concentration response functions – at least when odor signals are weak enough to avoid saturating PNs.

Conversely, when odor signals are strong, higher brain regions might rely preferentially on glomeruli that are sensitive to inhibition. This is because lateral inhibition prevents saturation in these glomeruli. In this way, inhibition can improve stimulus discrimination (Olsen et al., 2010; Luo et al., 2010).

Importantly, we show here that one odor tends to simultaneously activate glomerular channels that are sensitive and insensitive to inhibition. These different sorts of glomeruli thus represent parallel channels encoding the same signal. Our results are reminiscent of a recent study reporting that a visual stimulus simultaneously activates two types of retinal ganglion cells, one which adapts and one which shows anti-adaptation (Kastner and Baccus, 2011). There is also precedent for the idea that behaviors might correlate with certain glomeruli under particular conditions, but different glomeruli under other conditions. For example, in the *Drosophila* larva, one glomerulus drives behavioral responses to ethyl acetate at low concentrations, whereas another glomerulus drives responses to high concentrations, even though high concentrations co-activate both glomeruli (Kreher et al., 2008).

In sum, our results are a departure from the classic idea of selectivity in inhibitory circuits. Classically, inhibition is understood as stimulus-specific, because inhibition is often strongest between neurons having the same preferred stimuli, and target neurons are assumed to have uniform sensitivity to inhibition. This statement characterizes the classic case of topographic neural circuits. Our results illustrate a case of a non-topographic circuit where recruitment of inhibition is fairly nonspecific, but target neurons nonetheless have specific sensitivities to inhibition. We propose that this organization may find parallels in other neural circuits, and that it may represent a way to effectively implement lateral inhibition while minimizing some of the associated problems – namely, noise and ambiguity. This proposal is supported by the recent finding that neighboring pyramidal neurons in mammalian cortex can have dramatically different levels of total inhibitory synaptic drive (Xue et al., 2014). Our findings illustrate how tradeoffs in information processing can be resolved by allowing a stimulus to be encoded in parallel by individual neurons having different types of network interactions. This is an example of how neural population diversity can allow problems in neural computation to be resolved using simple parts (Marder and Goaillard, 2006).

EXPERIMENTAL PROCEDURES

Flies

All experiments were performed on female flies 2–3 days post-eclosion, with the exception of calcium imaging experiments, which were performed in older flies (see Supplemental Experimental Procedures), and experiments done in the *shakB²* background, which were performed in males. Genotypes used for each figure are as follows (see Supplemental Experimental Procedures for further information regarding each transgene):

Figure 1: (A–B) *pebbled-Gal4; UAS-GCaMP3.0.* (C–D) *UAS-GCaMP3.0; NP3056-Gal4/TM6B.* (E) pooled from *UAS-GCaMP3.0/SM6; NP3056-Gal4*, and *UAS-GCaMP3.0; NP3056-Gal4/TM6B*, and *UAS-GCaMP3.0/SM6; GH298-Gal4*, and *UAS-GCaMP3.0; GH298-Gal4/TM6B.*

Figure 2: (A–B) *UAS-GCaMP3.0; NP3056-Gal4/TM6B* (C) pooled from *UAS-GCaMP3.0/SM6; NP3056-Gal4*, and *UAS-GCaMP3.0; NP3056-Gal4/TM6B*, and *UAS-GCaMP3.0/SM6; GH298-Gal4*, and *UAS-GCaMP3.0; GH298-Gal4/TM6B.*

Figure 3: (A–B) *UAS-GCaMP3.0; GH298-Gal4/TM6B.* Note that transgenes were not used in (B) (C–E) pooled from *UAS-GCaMP3.0; GH298-Gal4/TM6B* and *UAS-GCaMP3.0; NP3056-Gal4/TM6B.*)

Figure 4: (A–B) +ChR: *UAS-GCaMP3.0/UAS-ChR2:YFP-C; NP3056-Gal4* and −ChR: *UAS-GCaMP3.0/SM6; NP3056-Gal4* (C–D) *shakB²/Y; UAS-ChR2:YFP-C/SM6; UAS-ChR2:YFP-B/NP3056-Gal4.* (E–F) *shakB²/Y; UAS-ChR2:YFP-C/SM6; UAS-ChR2:YFP-B/NP3056-Gal4* (ChR+ condition) or *shakB²/Y; UAS-ChR2:YFP-C/SM6; UAS-ChR2:YFP-B/TM6B.* (no Gal4 control, ChR-condition)

Figure 5: *shakB²/Y; UAS-ChR2:YFP-C/SM6; UAS-ChR2:YFP-B/NP3056-Gal4.*

Figure 6: (A–B) *UAS-bruchpilot:GFP/SM6; NP3056-Gal4/+*

Figure 7: *w^{1118}*

Figure 8: (A–C) pooled from *GH146-Gal4, UAS-CD8:GFP* (II) and *Mz19-Gal4, UAS-CD8:GFP* (II), and *NP3481-Gal4, UAS-CD8:GFP* (X), and *GMR46E07-Gal4/UAS-CD8:GFP* (III), and *w^{1118}*.

We also examined the expression pattern of Gal4 in a *Gad1–Gal4* line which was used in a prior study to evaluate spatial patterns of LN activity (Ng et al., 2002). We found that this Gal4 line labels PNs as well as LNs (Figure S5, see also Supplemental Experimental Procedures), which may contribute to why Ng et al. obtained results that are different from our calcium imaging results.

Odor delivery

All odor concentrations are reported as v/v dilutions in a solvent of paraffin oil. Odors were delivered essentially as previously described (Bhandawat et al., 2007) with minor modifications. The order of odor stimuli was independently randomized in each experiment, except for the concentration series experiments, where different concentrations of the same odor were always presented from least to most concentrated. The odor delivery tube was

flushed with clean air for 2 minutes when changing between odors. See Supplemental Experimental Procedures for details.

Calcium imaging of odor-evoked activity

The antennal lobes were imaged *in vivo* from the dorsal side while constantly perfusing the brain with oxygenated saline. GCaMP3 fluorescence was imaged using a 2-photon microscope at a frame rate of 7.8 Hz. By imaging odor-evoked calcium signals in ORN axon terminals, we identified four horizontal imaging planes (-12 μm, -24 μm, -36 μm, -48 μm relative to the dorsal surface of the antennal lobe neuropil) which collectively cover all the glomeruli activated by any of the "private" odors we used. We therefore focused our experiments on these four imaging planes, and we typically sampled two of these plane within the time constraints of each individual experiment. See Supplemental Experimental Procedures for details.

Calcium imaging of optogenetically-evoked activity

Optogenetically-evoked activity and odor-evoked activity were imaged in essentially the same manner. ChR2 was excited with light delivered from a fiber optic cannula coupled to an LED, with the tip of the cannula positioned above the antennal lobe. Light intensity was modulated by varying the voltage to the LED. See Supplemental Experimental Procedures for details.

Local field potential recordings

See Supplemental Experimental Procedures.

Immunohistochemistry

Biocytin fills were processed as previously described (Wilson et al., 2004). Both biocytin fills and LN anatomical data were acquired from fixed brains using a laser scanning confocal microscope. Fluorescence arising from LNs (bruchpilot:GFP, n-synaptobrevin:GFP signal, or cytoplasmic GFP) originates from direct fluorescence of the protein without amplification from immunostaining. See Supplemental Experimental Procedures for details.

Electrophysiology

In vivo whole-cell patch-clamp recordings were performed under visual control as previously described (Wilson et al., 2004). See Supplemental Experimental Procedures for details.

Optogenetics and light calibration

Flies used for optogenetic experiments were cultured on medium supplemented with all-trans-retinal. In Figures 4–5, excitation of ChR2 was achieved by delivering blue light through a 40× water-immersion objective, and power density was modulated using a fine series of neutral density filters. See Supplemental Experimental Procedures for details.

GABA uncaging

The experimental preparation and solutions were shielded from room lights. We verified that wash-in of DPNI-caged GABA did not change spontaneous synaptic activity. GABA was uncaged using UV light delivered through a 40× water-immersion objective. Power density was modulated using neutral density filters. In a subset of experiments, we confirmed that GABA receptor antagonists abolished the effect of light on sEPSC activity. We found no systematic relationship between glomerular depth and sensitivity to GABA. See Supplemental Experimental Procedures for details.

Analysis

See Supplemental Experimental Procedures for descriptions of principal component analysis (PCA), analysis of GCaMP3 F/F within specific glomeruli, analysis of LN anatomical data, quantification of sEPSC suppression, quantification of ORN odor selectivity, and general statistical methods. Data from glomerulus VC3 was excluded from our analyses because the odor tuning of VC3 PNs varied dramatically across experimental replicates (see Supplemental Experimental Procedures). Data for all glomerulus-by-glomerulus measurements in this study are provided in Supplemental Table 1.

Supplementary Material

Refer to Web version on PubMed Central for supplementary material.

Acknowledgements

REFERENCES

Abbott LF, Varela JA, Sen K, Nelson SB. Synaptic depression and cortical gain control. Science. 1997; 275:220–224. [PubMed: 8985017]

Ai M, Min S, Grosjean Y, Leblanc C, Bell R, Benton R, Suh GS. Acid sensing by the Drosophila olfactory system. Nature. 2010; 468:691–695. [PubMed: 21085119]

Asahina K, Louis M, Piccinotti S, Vosshall LB. A circuit supporting concentration-invariant odor perception in Drosophila. J Biol. 2009; 8:9. [PubMed: 19171076]

Bandyopadhyay S, Shamma SA, Kanold PO. Dichotomy of functional organization in the mouse auditory cortex. Nat Neurosci. 2010; 13:361–368. [PubMed: 20118924]

Barlow, HG. Possible principles underlying the transformation of sensory messages. In. In: Rosenblith, WA., editor. Sensory Communication. Cambridge, MA: MIT Press; 1961. p. 217-234.

Bhandawat V, Olsen SR, Schlief ML, Gouwens NW, Wilson RI. Sensory processing in the Drosophila antennal lobe increases the reliability and separability of ensemble odor representations. Nat. Neurosci. 2007; 10:1474–1482. [PubMed: 17922008]

Bock DD, Lee WC, Kerlin AM, Andermann ML, Hood G, Wetzel AW, Yurgenson S, Soucy ER, Kim HS, Reid RC. Network anatomy and in vivo physiology of visual cortical neurons. Nature. 2011; 471:177–182. [PubMed: 21390124]

Briggman KL, Helmstaedter M, Denk W. Wiring specificity in the direction-selectivity circuit of the retina. Nature. 2011; 471:183–188. [PubMed: 21390125]

Chou YH, Spletter ML, Yaksi E, Leong JC, Wilson RI, Luo L. Diversity and wiring variability of olfactory local interneurons in the Drosophila antennal lobe. Nat Neurosci. 2010; 13:439–449. [PubMed: 20139975]

Christensen TA, D'Alessandro G, Lega J, Hildebrand JG. Morphometric modeling of olfactory circuits in the insect antennal lobe: I. Simulations of spiking local interneurons. Biosystems. 2001; 61:143–153. [PubMed: 11716974]

Cleland TA, Johnson BA, Leon M, Linster C. Relational representation in the olfactory system. Proc Natl Acad Sci U S A. 2007; 104:1953–1958. [PubMed: 17261800]

Cleland TA. Construction of odor representations by olfactory bulb microcircuits. Prog Brain Res. 2014; 208:177–203. [PubMed: 24767483]

Clyne P, Grant A, O'Connell R, Carlson JR. Odorant response of individual sensilla on the Drosophila antenna. Invert. Neurosci. 1997; 3:127–135. [PubMed: 9783438]

Couto A, Alenius M, Dickson BJ. Molecular, anatomical, and functional organization of the Drosophila olfactory system. Curr. Biol. 2005; 15:1535–1547. [PubMed: 16139208]

Das A, Sen S, Lichtneckert R, Okada R, Ito K, Rodrigues V, Reichert H. Drosophila olfactory local interneurons and projection neurons derive from a common neuroblast lineage specified by the empty spiracles gene. Neural Dev. 2008; 3:33. [PubMed: 19055770]

de Bruyne M, Foster K, Carlson JR. Odor coding in the Drosophila antenna. Neuron. 2001; 30:537–552. [PubMed: 11395013]

Dudai Y. Properties of learning and memory in Drosophila melanogaster. J. Comp. Physiol. [A]. 1977; 114:69–89.

Dunn FA, Rieke F. Single-photon absorptions evoke synaptic depression in the retina to extend the operational range of rod vision. Neuron. 2008; 57:894–904. [PubMed: 18367090]

Fantana AL, Soucy ER, Meister M. Rat olfactory bulb mitral cells receive sparse glomerular inputs. Neuron. 2008; 59:802–814. [PubMed: 18786363]

Fishilevich E, Vosshall LB. Genetic and functional subdivision of the Drosophila antennal lobe. Curr. Biol. 2005; 15:1548–1553. [PubMed: 16139209]

Friedrich RW. Neuronal computations in the olfactory system of zebrafish. Annu Rev Neurosci. 2013; 36:383–402. [PubMed: 23725002]

Gibson JR, Beierlein M, Connors BW. Two networks of electrically coupled inhibitory neurons in neocortex. Nature. 1999; 402:75–79. [PubMed: 10573419]

Girardin CC, Kreissl S, Galizia CG. Inhibitory connections in the honeybee antennal lobe are spatially patchy. J Neurophysiol. 2013; 109:332–343. [PubMed: 23100135]

Grosjean Y, Rytz R, Farine JP, Abuin L, Cortot J, Jefferis GS, Benton R. An olfactory receptor for food-derived odours promotes male courtship in Drosophila. Nature. 2011; 478:236–240. [PubMed: 21964331]

Haddad R, Weiss T, Khan R, Nadler B, Mandairon N, Bensafi M, Schneidman E, Sobel N. Global features of neural activity in the olfactory system form a parallel code that predicts olfactory behavior and perception. J Neurosci. 2010; 30:9017–9026. [PubMed: 20610736]

Hallem EA, Carlson JR. Coding of odors by a receptor repertoire. Cell. 2006; 125:143–160. [PubMed: 16615896]

Huang J, Zhang W, Qiao W, Hu A, Wang Z. Functional connectivity and selective odor responses of excitatory local interneurons in Drosophila antennal lobe. Neuron. 2010; 67:1021–1033. [PubMed: 20869598]

Husch A, Paehler M, Fusca D, Paeger L, Kloppenburg P. Distinct electrophysiological properties in subtypes of nonspiking olfactory local interneurons correlate with their cell type-specific Ca2+ current profiles. J Neurophysiol. 2009; 102:2834–2845. [PubMed: 19759323]

Isaacson JS, Scanziani M. How inhibition shapes cortical activity. Neuron. 2011; 72:231–243. [PubMed: 22017986]

Kaas JH. Topographic maps are fundamental to sensory processing. Brain Res Bull. 1997; 44:107–112. [PubMed: 9292198]

Kastner DB, Baccus SA. Coordinated dynamic encoding in the retina using opposing forms of plasticity. Nat Neurosci. 2011; 14:1317–1322. [PubMed: 21909086]

Kazama H, Wilson RI. Homeostatic matching and nonlinear amplification at genetically-identified central synapses. Neuron. 2008; 58:401–413. [PubMed: 18466750]

Kazama H, Wilson RI. Origins of correlated activity in an olfactory circuit. Nat. Neurosci. 2009 in press.

Kreher SA, Mathew D, Kim J, Carlson JR. Translation of sensory input into behavioral output via an olfactory system. Neuron. 2008; 59:110–124. [PubMed: 18614033]

Liu BH, Li YT, Ma WP, Pan CJ, Zhang LI, Tao HW. Broad inhibition sharpens orientation selectivity by expanding input dynamic range in mouse simple cells. Neuron. 2011; 71:542–554. [PubMed: 21835349]

Luo M, Katz LC. Response correlation maps of neurons in the mammalian olfactory bulb. Neuron. 2001; 32:1165–1179. [PubMed: 11754845]

Luo SX, Axel R, Abbott LF. Generating sparse and selective third-order responses in the olfactory system of the fly. Proc Natl Acad Sci U S A. 2010; 107:10713–10718. [PubMed: 20498080]

Marder E, Goaillard JM. Variability, compensation and homeostasis in neuron and network function. Nat. Rev. Neurosci. 2006; 7:563–574. [PubMed: 16791145]

Ng M, Roorda RD, Lima SQ, Zemelman BV, Morcillo P, Miesenbock G. Transmission of olfactory information between three populations of neurons in the antennal lobe of the fly. Neuron. 2002; 36:463–474. [PubMed: 12408848]

Ohki K, Chung S, Ch'ng YH, Kara P, Reid RC. Functional imaging with cellular resolution reveals precise micro-architecture in visual cortex. Nature. 2005; 433:597–603. [PubMed: 15660108]

Okada R, Awasaki T, Ito K. Gamma-aminobuyric acid (GABA)-mediated neural connections in the Drosophila antennal lobe. J. Comp. Neurol. 2009; 514:74–91. [PubMed: 19260068]

Olsen SR, Wilson RI. Lateral presynaptic inhibition mediates gain control in an olfactory circuit. Nature. 2008; 452:956–960. [PubMed: 18344978]

Olsen SR, Bhandawat V, Wilson RI. Divisive normalization in olfactory population codes. Neuron. 2010; 66:287–299. [PubMed: 20435004]

Poo C, Isaacson JS. Odor representations in olfactory cortex: "sparse" coding, global inhibition, and oscillations. Neuron. 2009; 62:850–861. [PubMed: 19555653]

Redish AD, Battaglia FP, Chawla MK, Ekstrom AD, Gerrard JL, Lipa P, Rosenzweig ES, Worley PF, Guzowski JF, McNaughton BL, Barnes CA. Independence of firing correlates of anatomically proximate hippocampal pyramidal cells. J Neurosci. 2001; 21:RC134. [PubMed: 11222672]

Rieke F, Rudd ME. The challenges natural images pose for visual adaptation. Neuron. 2009; 64:605–616. [PubMed: 20005818]

Root CM, Masuyama K, Green DS, Enell LE, Nassel DR, Lee CH, Wang JW. A presynaptic gain control mechanism fine-tunes olfactory behavior. Neuron. 2008; 59:311–321. [PubMed: 18667158]

Rothschild G, Nelken I, Mizrahi A. Functional organization and population dynamics in the mouse primary auditory cortex. Nat Neurosci. 2010; 13:353–360. [PubMed: 20118927]

Sachse S, Galizia CG. Role of inhibition for temporal and spatial odor representation in olfactory output neurons: a calcium imaging study. J. Neurophysiol. 2002; 87:1106–1117. [PubMed: 11826074]

Schlief ML, Wilson RI. Olfactory processing and behavior downstream from highly selective receptor neurons. Nat. Neurosci. 2007; 10:623–630. [PubMed: 17417635]

Seki Y, Rybak J, Wicher D, Sachse S, Hansson BS. Physiological and morphological characterization of local interneurons in the Drosophila antennal lobe. J Neurophysiol. 2010; 104:1007–1019. [PubMed: 20505124]

Shepherd, GM., Greer, CA. Olfactory bulb. In: Shepherd, GM., editor. The Synaptic Organization of the Brain. New York: Oxford University Press; 1998. p. 159-203.

Silbering AF, Galizia CG. Processing of odor mixtures in the Drosophila antennal lobe reveals both global inhibition and glomerulus-specific interactions. J. Neurosci. 2007; 27:11966–11977. [PubMed: 17978037]

Silbering AF, Okada R, Ito K, Galizia CG. Olfactory information processing in the Drosophila antennal lobe: anything goes? J Neurosci. 2008; 28:13075–13087. [PubMed: 19052198]

Silbering AF, Rytz R, Grosjean Y, Abuin L, Ramdya P, Jefferis GS, Benton R. Complementary function and integrated wiring of the evolutionarily distinct Drosophila olfactory subsystems. J Neurosci. 2011; 31:13357–13375. [PubMed: 21940430]

Soucy ER, Albeanu DF, Fantana AL, Murthy VN, Meister M. Precision and diversity in an odor map on the olfactory bulb. Nat. Neurosci. 2009; 12:210–220. [PubMed: 19151709]

Srinivasan MV, Laughlin SB, Dubs A. Predictive coding: a fresh view of inhibition in the retina. Proc R Soc Lond B Biol Sci. 1982; 216:427–459. [PubMed: 6129637]

Stensmyr MC, Dweck HK, Farhan A, Ibba I, Strutz A, Mukunda L, Linz J, Grabe V, Steck K, Lavista-Llanos S, et al. A conserved dedicated olfactory circuit for detecting harmful microbes in Drosophila. Cell. 2012; 151:1345–1357. [PubMed: 23217715]

Stettler DD, Axel R. Representations of odor in the piriform cortex. Neuron. 2009; 63:854–864. [PubMed: 19778513]

Suh GS, Wong AM, Hergarden AC, Wang JW, Simon AF, Benzer S, Axel R, Anderson DJ. A single population of olfactory sensory neurons mediates an innate avoidance behaviour in Drosophila. Nature. 2004; 431:854–859. [PubMed: 15372051]

Tian L, Hires SA, Mao T, Huber D, Chiappe ME, Chalasani SH, Petreanu L, Akerboom J, McKinney SA, Schreiter ER, et al. Imaging neural activity in worms, flies and mice with improved GCaMP calcium indicators. Nat Methods. 2009; 6:875–881. [PubMed: 19898485]

Trigo FF, Corrie JE, Ogden D. Laser photolysis of caged compounds at 405 nm: photochemical advantages, localisation, phototoxicity and methods for calibration. J Neurosci Methods. 2009; 180:9–21. [PubMed: 19427524]

van der Goes van Naters W, Carlson JR. Receptors and neurons for fly odors in Drosophila. Curr. Biol. 2007; 17:606–612. [PubMed: 17363256]

Vidyasagar TR, Pei X, Volgushev M. Multiple mechanisms underlying the orientation selectivity of visual cortical neurones. Trends Neurosci. 1996; 19:272–277. [PubMed: 8799969]

Vinje WE, Gallant JL. Sparse coding and decorrelation in primary visual cortex during natural vision. Science. 2000; 287:1273–1276. [PubMed: 10678835]

Vosshall LB, Stocker RF. Molecular architecture of smell and taste in Drosophila. Annu Rev Neurosci. 2007; 30:505–533. [PubMed: 17506643]

Willhite DC, Nguyen KT, Masurkar AV, Greer CA, Shepherd GM, Chen WR. Viral tracing identifies distributed columnar organization in the olfactory bulb. Proc Natl Acad Sci U S A. 2006; 103:12592–12597. [PubMed: 16895993]

Wilson RI, Turner GC, Laurent G. Transformation of olfactory representations in the Drosophila antennal lobe. Science. 2004; 303:366–370. [PubMed: 14684826]

Wilson RI, Laurent G. Role of GABAergic inhibition in shaping odor-evoked spatiotemporal patterns in the Drosophila antennal lobe. J. Neurosci. 2005; 25:9069–9079. [PubMed: 16207866]

Wilson RI. Early olfactory processing in Drosophila: mechanisms and principles. Annu. Rev. Neurosci. 2013; 36 in press.

Wu GK, Arbuckle R, Liu BH, Tao HW, Zhang LI. Lateral sharpening of cortical frequency tuning by approximately balanced inhibition. Neuron. 2008; 58:132–143. [PubMed: 18400169]

Xue M, Atallah BV, Scanziani M. Equalizing excitation-inhibition ratios across visual cortical neurons. Nature. 2014; 511:596–600. [PubMed: 25043046]

Yaksi E, Wilson RI. Electrical coupling between olfactory glomeruli. Neuron. 2010; 67:1034–1047. [PubMed: 20869599]

Yao CA, Ignell R, Carlson JR. Chemosensory coding by neurons in the coeloconic sensilla of the Drosophila antenna. J. Neurosci. 2005; 25:8359–8367. [PubMed: 16162917]

Yarali A, Ehser S, Hapil FZ, Huang J, Gerber B. Odour intensity learning in fruit flies. Proc Biol Sci. 2009; 276:3413–3420. [PubMed: 19586944]

Yoshimura Y, Callaway EM. Fine-scale specificity of cortical networks depends on inhibitory cell type and connectivity. Nat Neurosci. 2005; 8:1552–1559. [PubMed: 16222228]
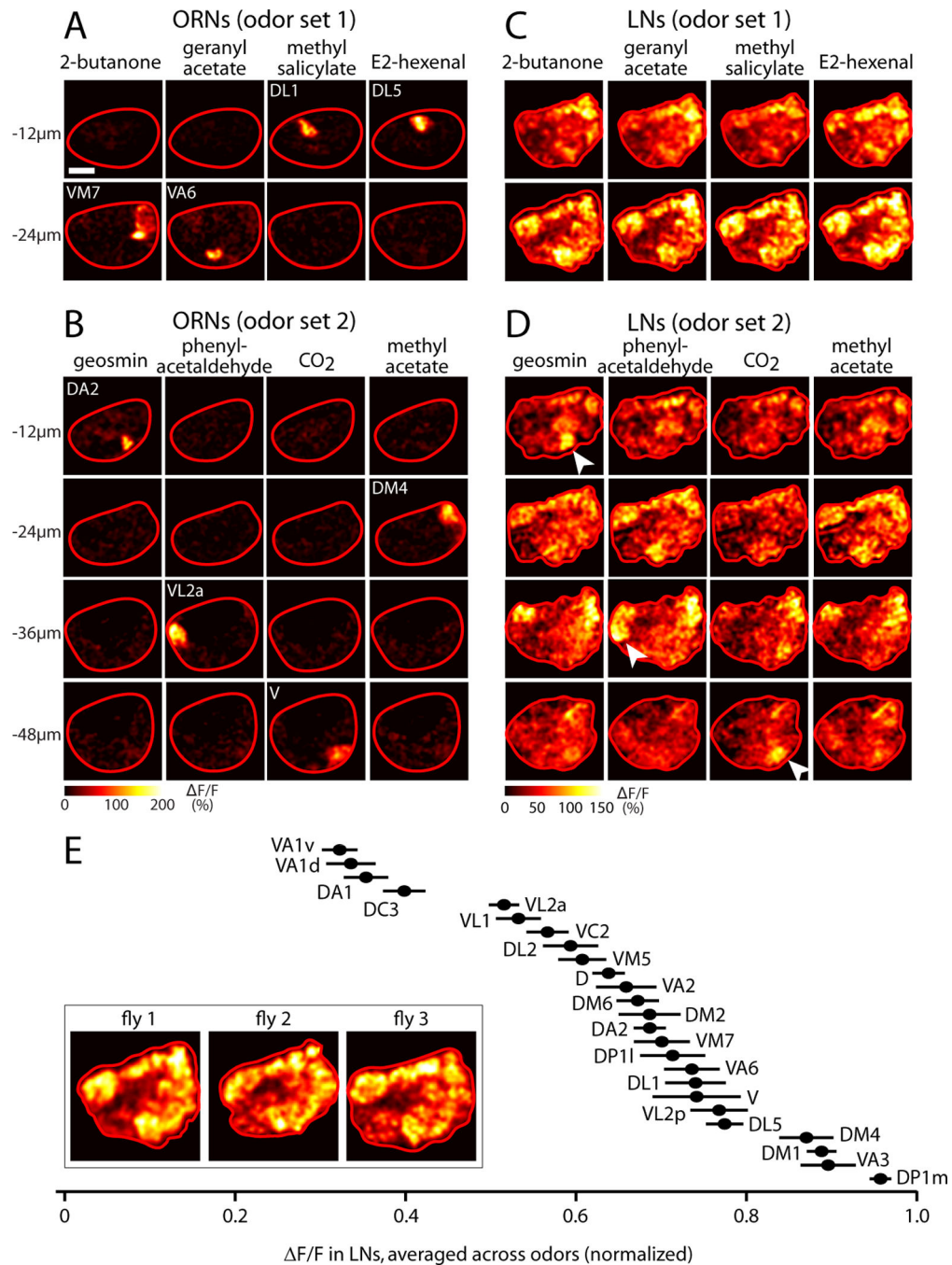
Figure 1. Activating a single glomerulus with odor recruits LN activity to all glomeruli

(A) Two-photon imaging of odor-evoked calcium signals in ORN axon terminals. GCaMP3 is expressed in ORNs under the control of *pebbled-Gal4*. The antennal lobe is viewed from the dorsal side and outlined in red (anterior is down, medial is right). Scale bar, 20 μm. Odors were largely "private," defined as activating only one ORN type. Odor set 1 is: 2-butanone, 5×10^{-6} (private for glomerulus VM7); geranyl acetate, 10^{-5} (VA6); methyl salicylate, 5×10^{-5} (DL1); E2-hexenal, 10^{-6} (DL5). Active glomeruli resided in two imaging planes, at −12μm (DL1 and DL5) and −24μm (VM7 and VA6).

(B) Same as (A) but for a different set of experiments using odor set 2: geosmin, 1% (DA2); phenylacetaldehyde, 10^{-5} (VL2a); CO_2, 5% (V); methyl acetate, 10^{-5} (DM4). Active glomeruli resided in four different imaging planes (-12 μm, -24 μm, -36 μm, -48 μm).

(C–D) Same as (A–B), but for GABAergic LNs. GCaMP3 is expressed under the control of *NP3056-Gal4*, but similar results were seen for *GH298-Gal4* (Figure S1). Activating individual glomeruli elicits a global pattern of LN activity. Imaging planes are selected to match the planes containing the glomeruli directly excited by these sets of odors, but similar results are seen in all planes. Note that three of the private odors in set 2 recruit extra LN activity in their cognate glomerulus (white arrowheads).

(E) The spatial pattern of LN activity is similar across individuals. Images were averaged across odors within each experiment, and LN activity was quantified in glomeruli that could be identified with confidence. The value for each glomerulus was normalized to the maximum glomerulus in that brain (n= 6–19 experiments, mean ± SEM). Across individuals, a given glomerulus exhibits a characteristic level of LN activity (one-way ANOVA, p=10^{-85}). Inset shows odoraveraged activity for three individual flies (GCaMP expressed under the control of *NP3056* for fly 1, *GH298* for flies 2 and 3); see Figure S1 for glomerular boundaries in this plane.
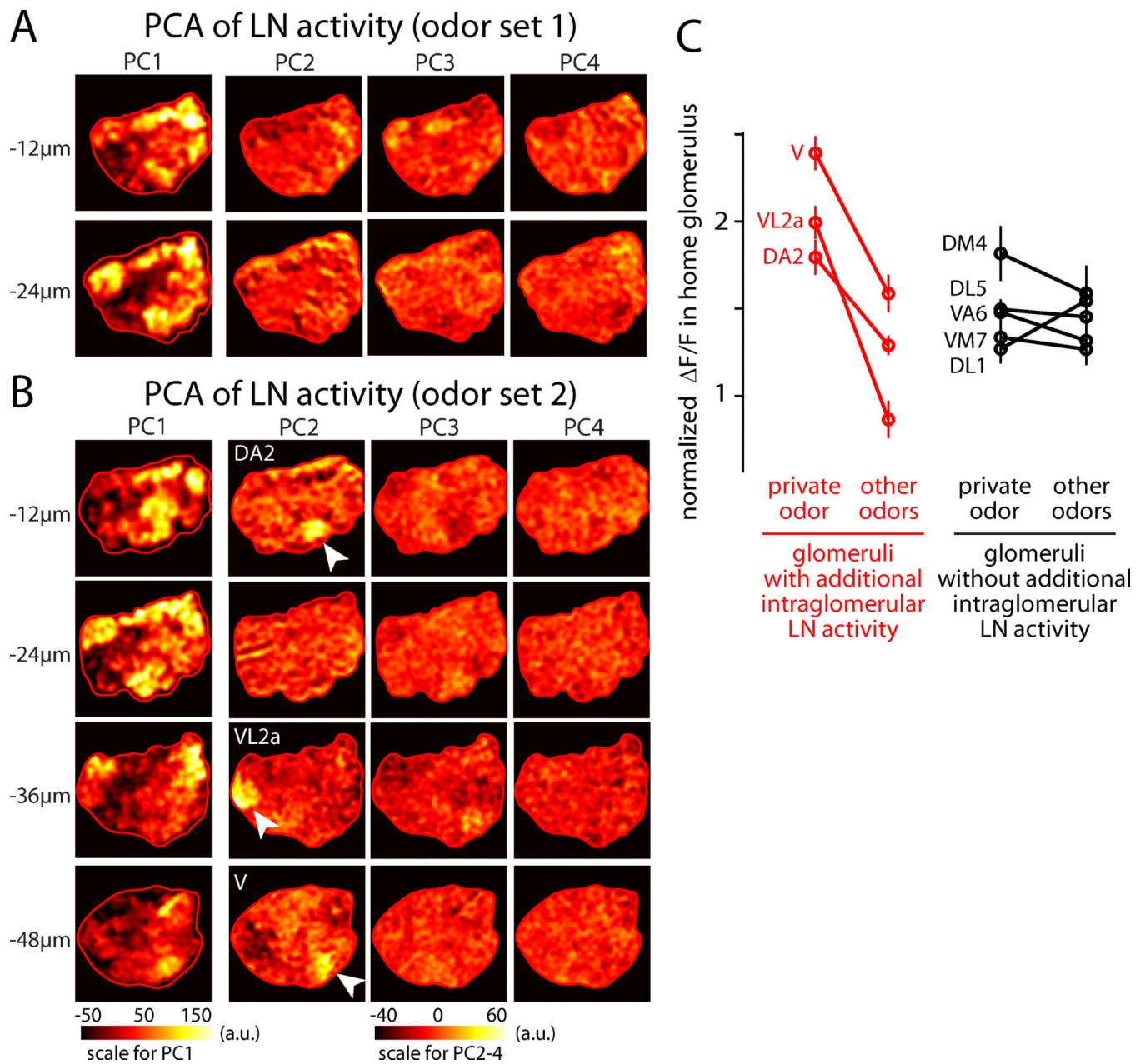
Figure 2. Activation of some glomeruli recruits intraglomerular LN activity in addition to the global pattern of LN activity

(A) Principal components of the LN activity patterns from Figure 1C (odor set 1). The input to each PCA is a set of four images, one for each of the four odors in the stimulus set. The output of the analysis is therefore four principal components (PCs). Overall, odor responses (in Figure 1C) resemble a scaled version of the first principal component (PC1). PCA was computed separately within each imaging plane and was applied only to the pixels contained in the antennal lobe (red ROI). Note the different color scale for PC1 compared to PC2–PC4.

(B) Same as above but for odor set 2. Overall, odor responses (in Figure 1D) resemble a scaled version of PC1. In addition, some odors in this set evoke additional activity in their cognate glomerulus (geosmin, phenylacetaldehyde, CO_2), and thus their cognate glomerulus

appears as PC2 in the corresponding imaging plane (DA2 for geosmin, VL2a for phenylacetaldehyde, V for CO_2). In the three imaging planes where these three glomeruli reside, they are indicated by arrowheads. The spatial structure of PC2 is reproducible across experiments (n=6–8 for odor set 2).

(C) LN activity in each of the eight glomeruli corresponding to our eight private odors. For each data point, F/F was measured in one glomerulus and then normalized to the average measured across the entire antennal lobe (mean of 6–13 experiments, ± SEM). For each glomerulus, the amount of activity elicited by its private odor was compared to the average activity elicited by the other three odors used in that experiment. For three glomeruli, there was a significant difference between the private odor and other odors (DA2, VL2a, V; p=0.003–0.01, p-values are Bonferroni-corrected for multiple comparisons). These were also the glomeruli which emerged as principal components in PCA (A–B). For the other glomeruli, there was no significant difference.
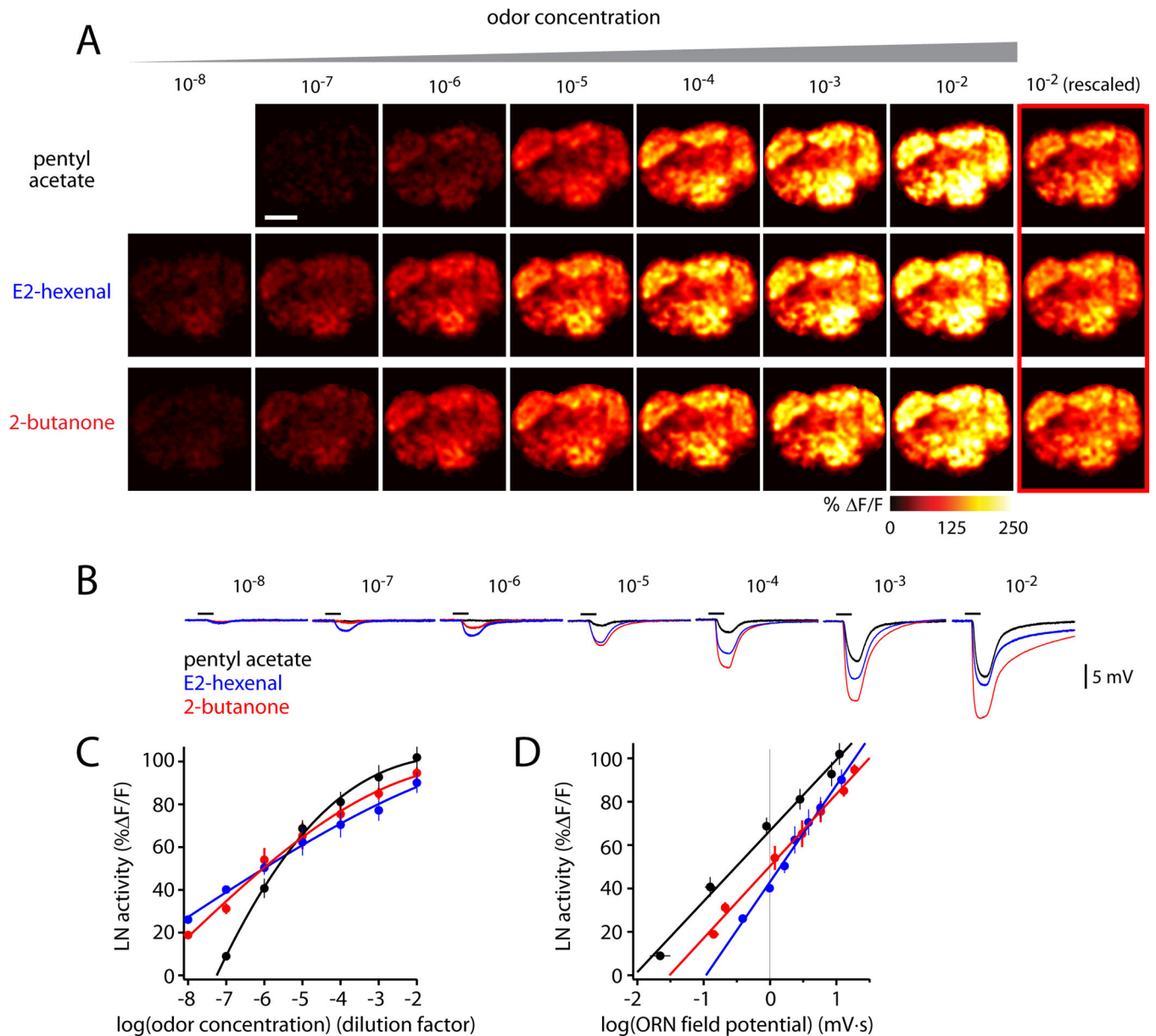
Figure 3. LN activity increases with total ORN input

(A) Odor-evoked calcium signals in LNs elicited by a family of concentrations for each odor. GCaMP3 is expressed under the control of *GH298-Gal4*. Note that the color scale differs from that in Figure 1. Scale bar, 20 μm. Different stimuli elicit similar spatial patterns of LN activity, but with different magnitudes. The last column (red outline) is the response to the highest concentration (10^{-2}) rescaled to match the response to an intermediate concentration (10^{-4}): note the similarity in spatial patterns.

(B) Local field potentials recorded in an antenna elicited by the same stimuli. The black bar is the 500-msec odor stimulus period.

(C) Overall levels of LN activity increase with odor concentration. For each concentration of each odor, LN activity (% F/F) was averaged across all glomeruli and experiments. Error bars are ± SEM across experiments. Lines are Hill equation fits. Either *GH298-Gal4* (5–7

experiments) or *NP3056-Gal4* (3 experiments) was used to drive GCaMP expression; the two data sets were pooled because results were similar.

(D) Overall levels of LN activity depend linearly on the logarithm of ORN input. LN data is the same as in (C). ORN input is measured by averaging local field potential recordings (8 antennal recordings like that in (B), averaged together with 5 palp recordings, each weighted according to the proportion of ORNs housed in each respective structure, ± SEM; see Supplemental Experimental Procedures). Analysis of covariance indicates a significant interaction between LN activity and odor across concentrations (p=0.002).
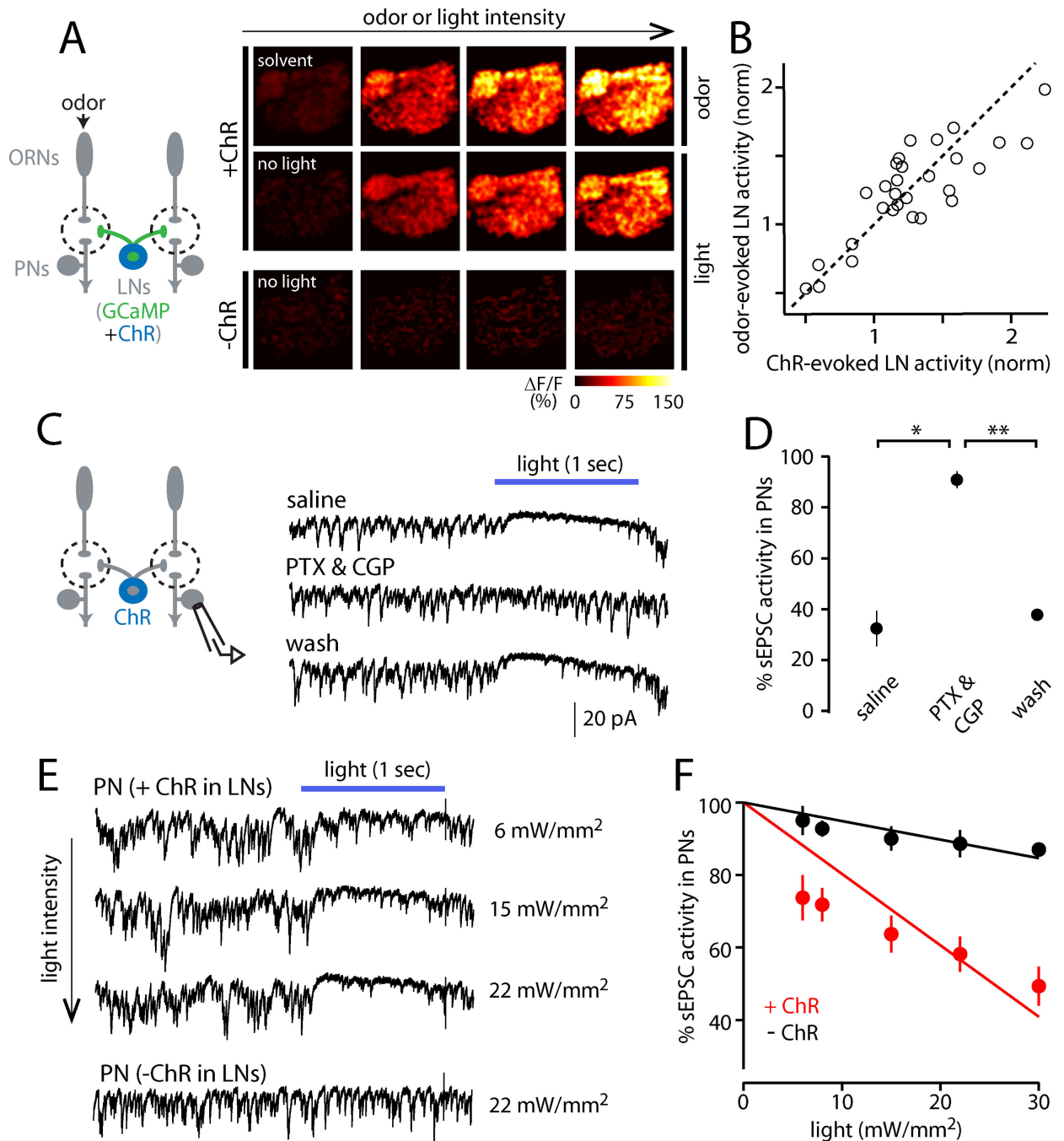
Figure 4. Optogenetic stimulation of LNs to measure PN sensitivity to inhibition

(**A**) Both GCaMP3 and channelrhodopsin-2 (ChR) were expressed in LNs. LNs were excited using either odor or light in the same brain. LN activity increases with increasing levels of odor (2-butanone) or light (470 nm). There were no light-evoked calcium signals without ChR (bottom).

(**B**) Each symbol compares the amount of LN activity evoked by odor versus light in a glomerulus in the same experiment (n=40 data points in 5 brains). Activity is normalized to the average amount of activity in the antennal lobe elicited by the respective stimulus. The

dotted line is unity. The correlation between odor- and light-evoked activity is strong and significant (R^2=0.80, p=10^{-14}), meaning the two methods produce the same spatial pattern.

(C) ChR-expressing LNs were excited using light while sEPSCs were recorded from a PN. Optogenetic excitation of LNs suppresses sEPSCs, and this effect is reversibly blocked by $GABA_A$ and $GABA_B$ receptor antagonists (5 μM picrotoxin and 50 μM CGP54626; light is 488 nm, 22 mW/mm^2).

(D) The effect of LN activity on sEPSCs is significantly different in GABA receptor antagonists than in saline or wash (*p=0.006, **p=0.002; paired t-tests, n=3). Open circles are individual cells; filled circles are mean ± SEM.

(E) Increasing light intensity produces increasing suppression of sEPSCs in a recording where LNs express ChR. Light has minimal effect without ChR (bottom row).

(F) Percent sEPSC activity versus light intensity for a representative cell from each genotype. This metric can range from 0 (full suppression) to 100 (no suppression); see Supplementary Experimental Procedures for details. Lines are fits constrained to intersect the y-axis at 100. Across a test set of PNs, the slopes of the fitted lines were significantly different between ChR-expressing and control flies (n=8 and 5, respectively, p=2×10^{-4}, unpaired t-test, data not shown).
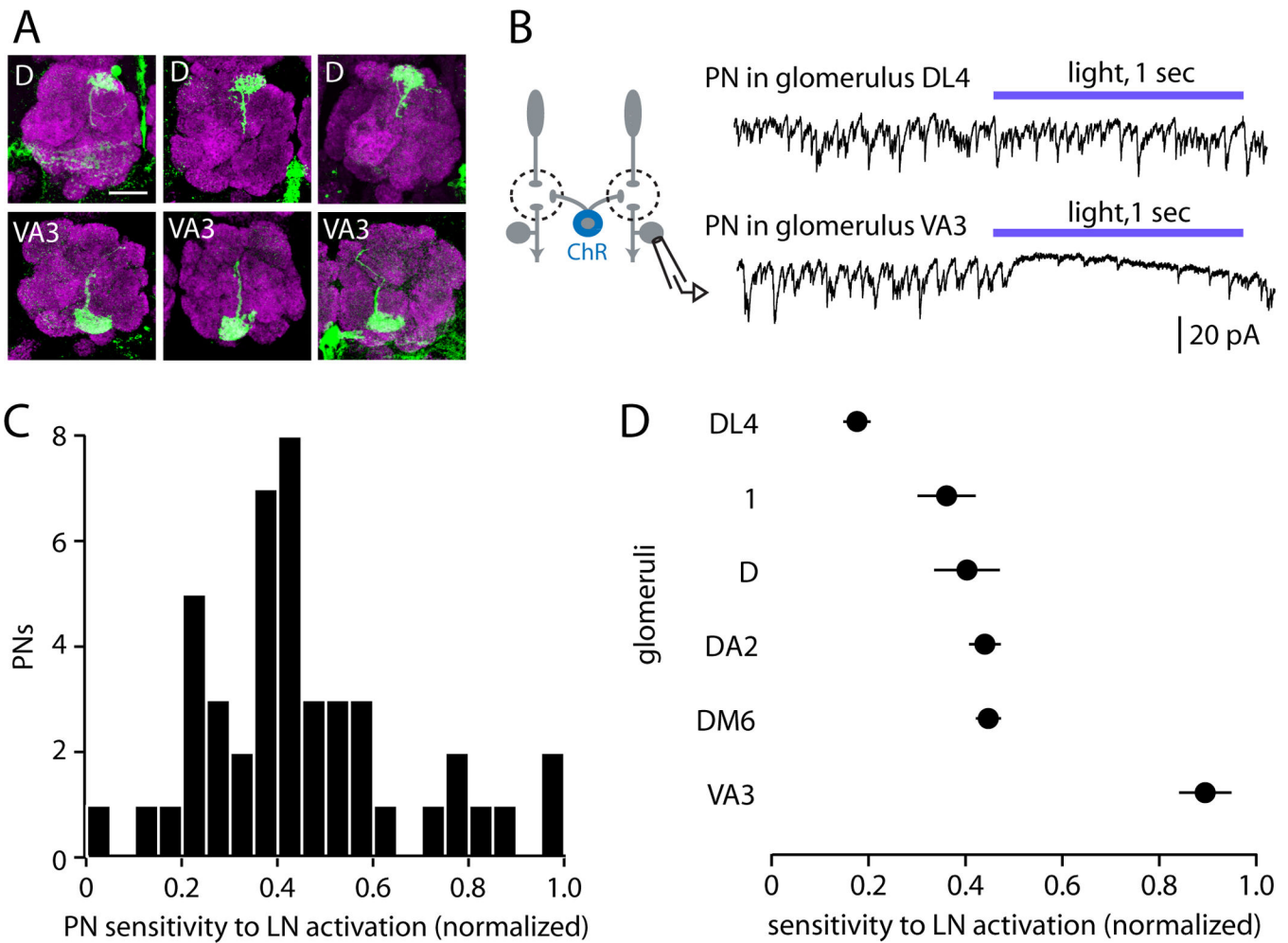
Figure 5. Glomeruli vary widely and stereotypically in their sensitivity to LN activation
(A) Examples of biocytin fills used to identify recorded PNs (green). Magenta is neuropil
(nc82 Ab) which marks glomerular boundaries. Scale bar, 20μm.

(B) Examples of PN responses to optogenetic activation of LNs. Sensitivity ranges from
nearly totally insensitive (e.g. glomerulus DL4) to almost completely inhibited (e.g.
glomerulus VA3). Light was delivered at 22 mW/mm^2.

(C) Sensitivity to LN activation for all recorded PNs (n=46). Sensitivity is measured as the
slope of the line fitted to the plot of percent sEPSC activity versus light intensity (see Figure
4F). Slopes are normalized across cells by setting the most negative slope (most inhibited) to
1.

(D) Sensitivity to LN activation for those glomeruli in which more than one PN was sampled
(2 – 6 PNs per glomerulus, mean ± SEM). PNs in the same glomerulus are significantly
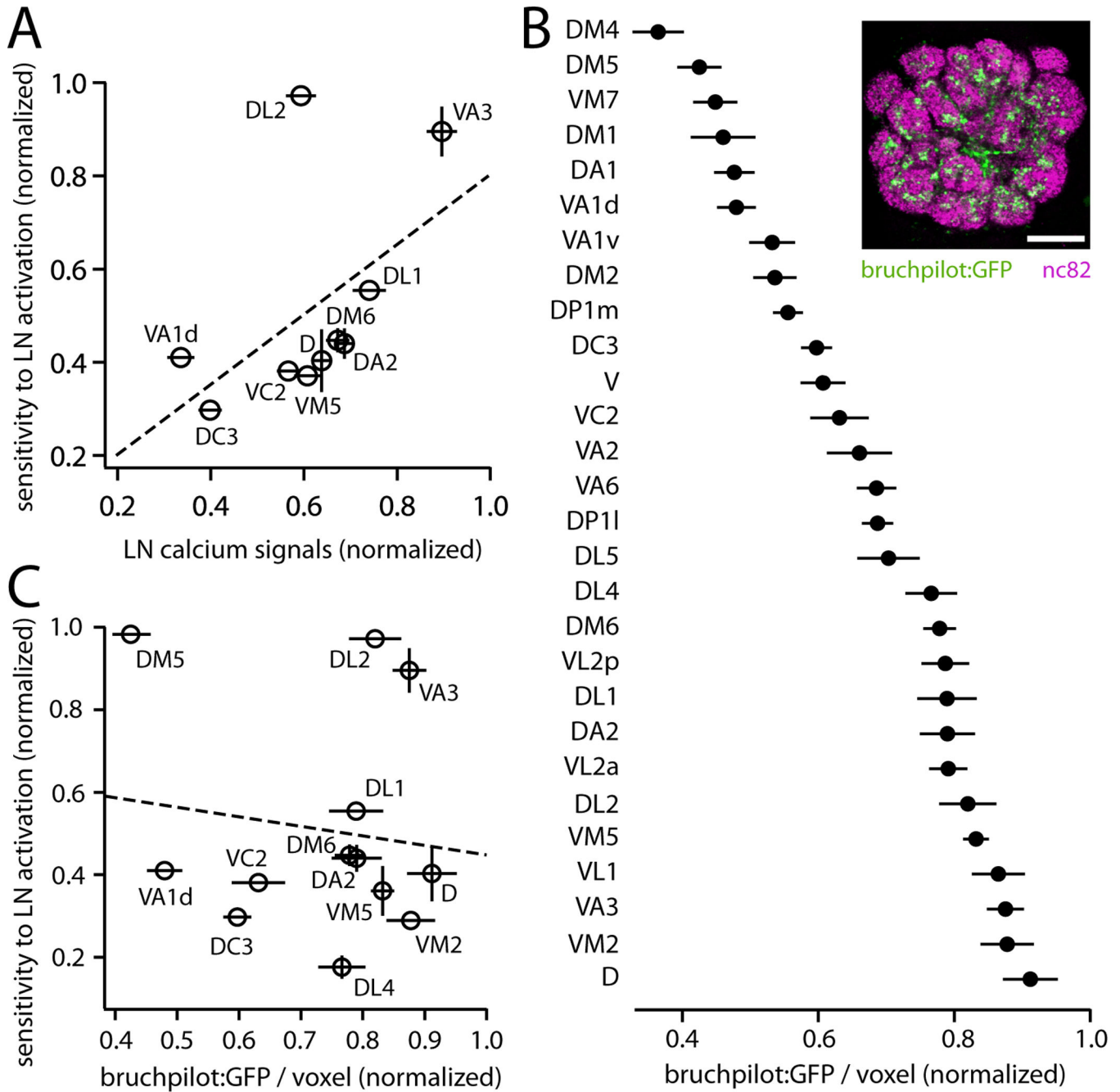more similar than those in different glomeruli (one-way ANOVA, p=8×10^{-6}).

Figure 6. The density of LN release sites does not predict sensitivity to LN activation

(A) Sensitivity to LN activation is not significantly correlated with LN calcium signals
(R^2=0.28, p=0.12).

(B) Inset: single confocal section through the antennal lobe of a fly expressing a marker of
presynaptic release sites (bruchpilot:GFP) in a large subset of LNs under the control of
NP3056-Gal4. Neuropil is immunostained (nc82 Ab) to visualize glomerular boundaries.
Scale bar, 20 μm. Graph shows measurements of bruchpilot:GFP signal per unit glomerular
volume, normalized within each brain to the glomerulus with the highest value. Data are the
mean of 6 measurements, ± SEM. The density of bruchpilot:GFP varies significantly across

glomeruli (one-way ANOVA, $p=10^{-36}$). Similar results were observed with two other markers of LN morphology (Figure S4).

(C) Sensitivity to LN activation (data from Figure 5C) is not correlated with the density of LN release sites ($R^2 = 0.02$, p = 0.67, permutation test).
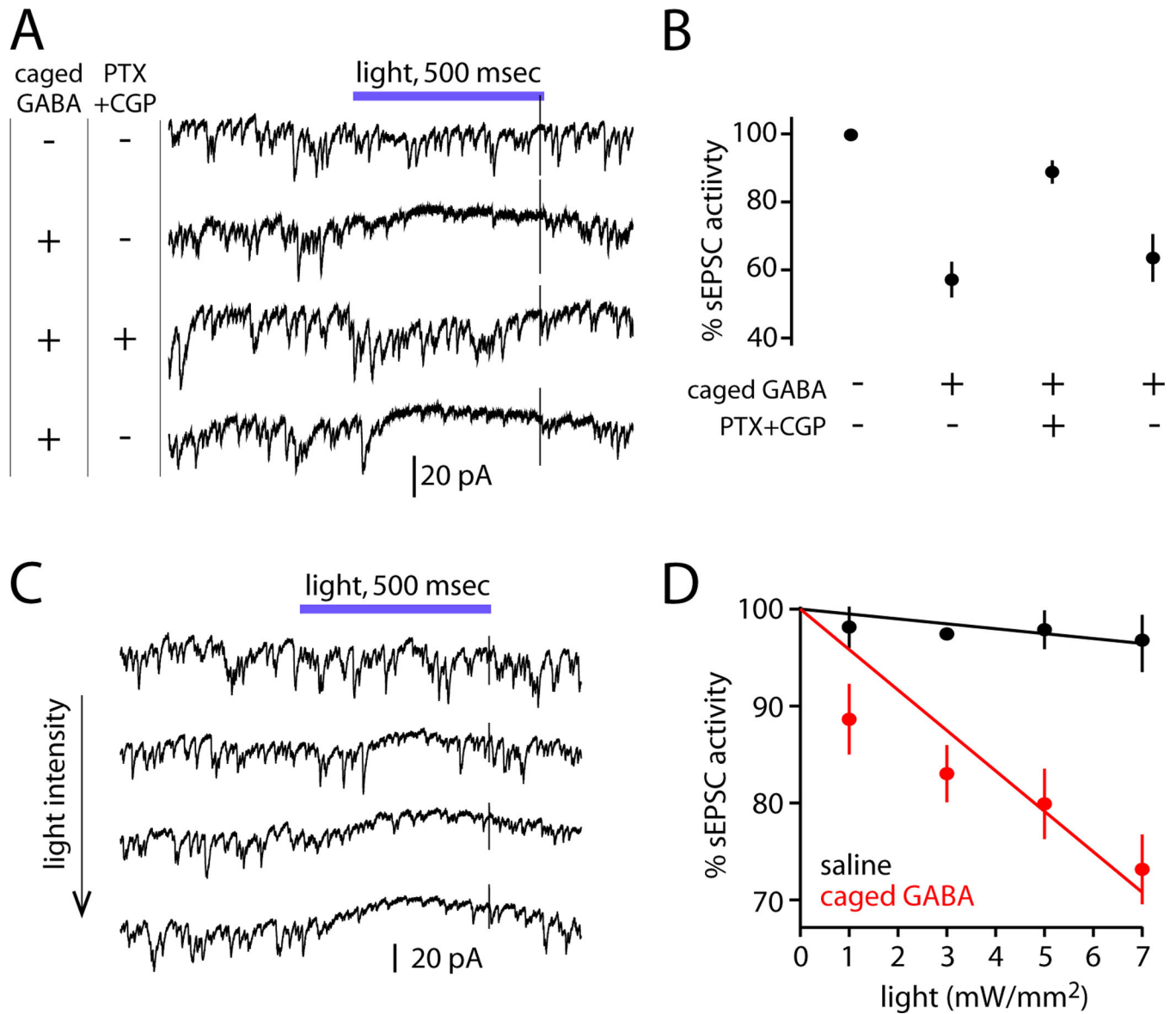
Figure 7. Evaluating GABA sensitivity using flash photolysis of caged GABA

(A) Full-field photolysis of DPNI-caged GABA (390 nm light, 7 mW/mm^2) transiently suppresses sEPSCs in a PN. Suppression is reversibly blocked by GABA receptor antagonists (5 μM picrotoxin, 50 μM CGP54626).

(B) Suppression requires caged GABA and functional GABA receptors (n=3, mean ± SEM). Light was delivered at 7–8 mW/mm^2.

(C) In the presence of caged GABA, sEPSCs are increasingly suppressed by higher light intensities.

(D) Percent sEPSC activity and fits are calculated as in Figure 4F. Data is shown from one representative cell in caged GABA and one in regular saline (mean ± SEM across trials). Across a test set of PNs, the slopes of the fitted lines were significantly different in saline versus caged GABA (n=5 and 7, p=10^{-4}, data not shown).
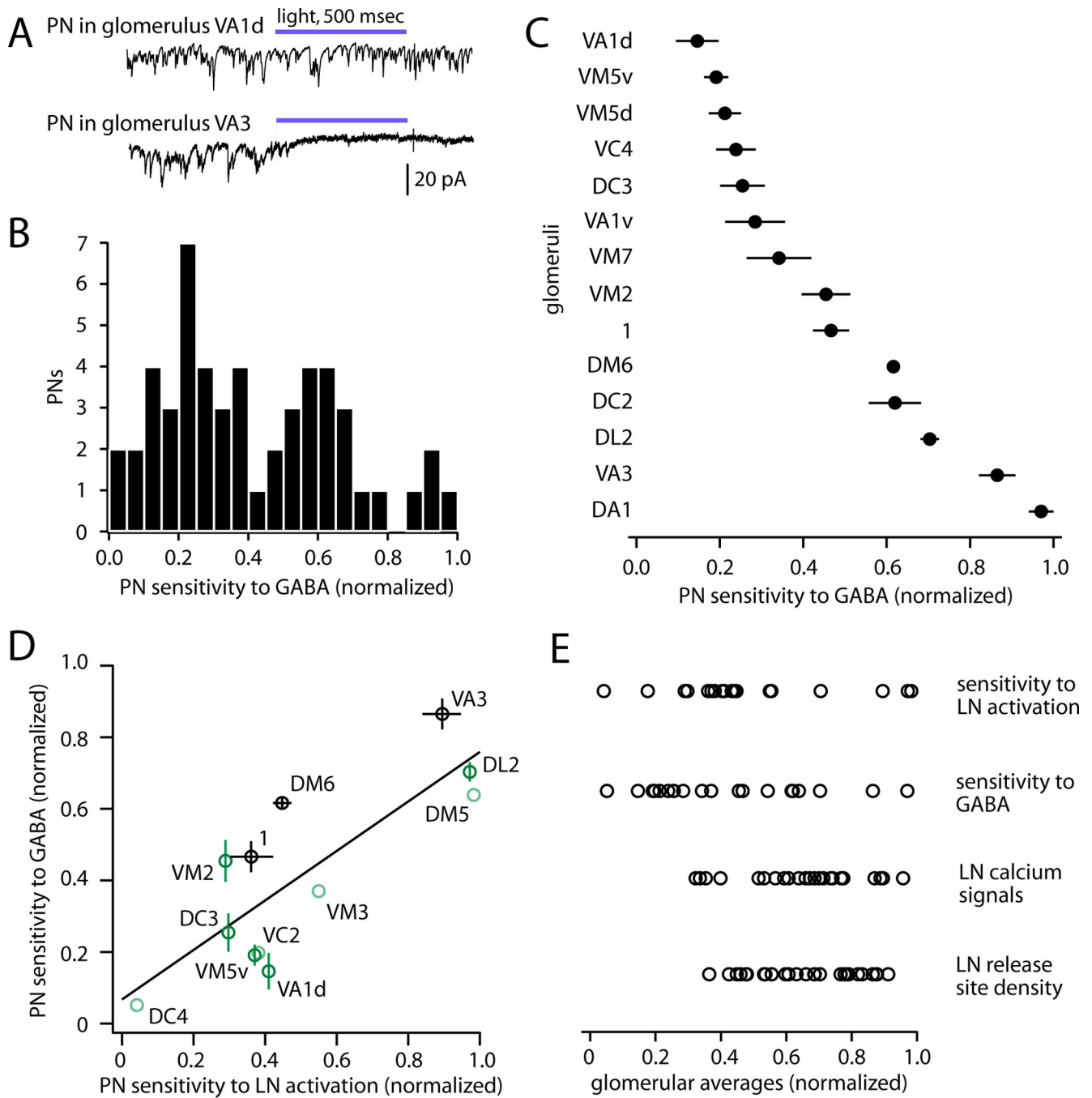
Figure 8. Sensitivity to LN activation is predicted by sensitivity to GABA

(A) Examples of PN responses to GABA uncaging. Sensitivity ranged from nearly completely insensitive (e.g., glomerulus VA1d) to nearly completely suppressed (e.g., glomerulus VA3). Light was delivered at 11 mW/mm^2.

(B) GABA sensitivity for all PNs (n=52). Sensitivity for each cell is measured as the slope of the line fitted to the plot of percent sEPSC activity versus light intensity (see Figure 7D). Slopes are normalized across cells by setting the most negative slope (most suppressed) to 1.

(C) GABA sensitivity of PNs for those glomeruli in which more than one PN was sampled (n=2–6 PNs per glomerulus, mean ± SEM). PNs in the same glomerulus are significantly more similar than those in different glomeruli (one-way ANOVA, p=10^{-9}).

(D) Sensitivity to GABA versus sensitivity to LN activation, for all glomeruli where both types of measurements are available (R^2=0.65, p=0.002, permutation test). Light green points are singly sampled for both measurements; dark green points are singly sampled for one measurement; and black points are sampled multiple times for both measurements. Error bars indicate SEM.

(E) Across glomeruli, sensitivity to LN activation and sensitivity to GABA vary over the same large range. By comparison, LN calcium signals (F/F, Figure 1) and LN release site density (Figure 6) span a narrower range. Each symbol represents a different glomerulus.
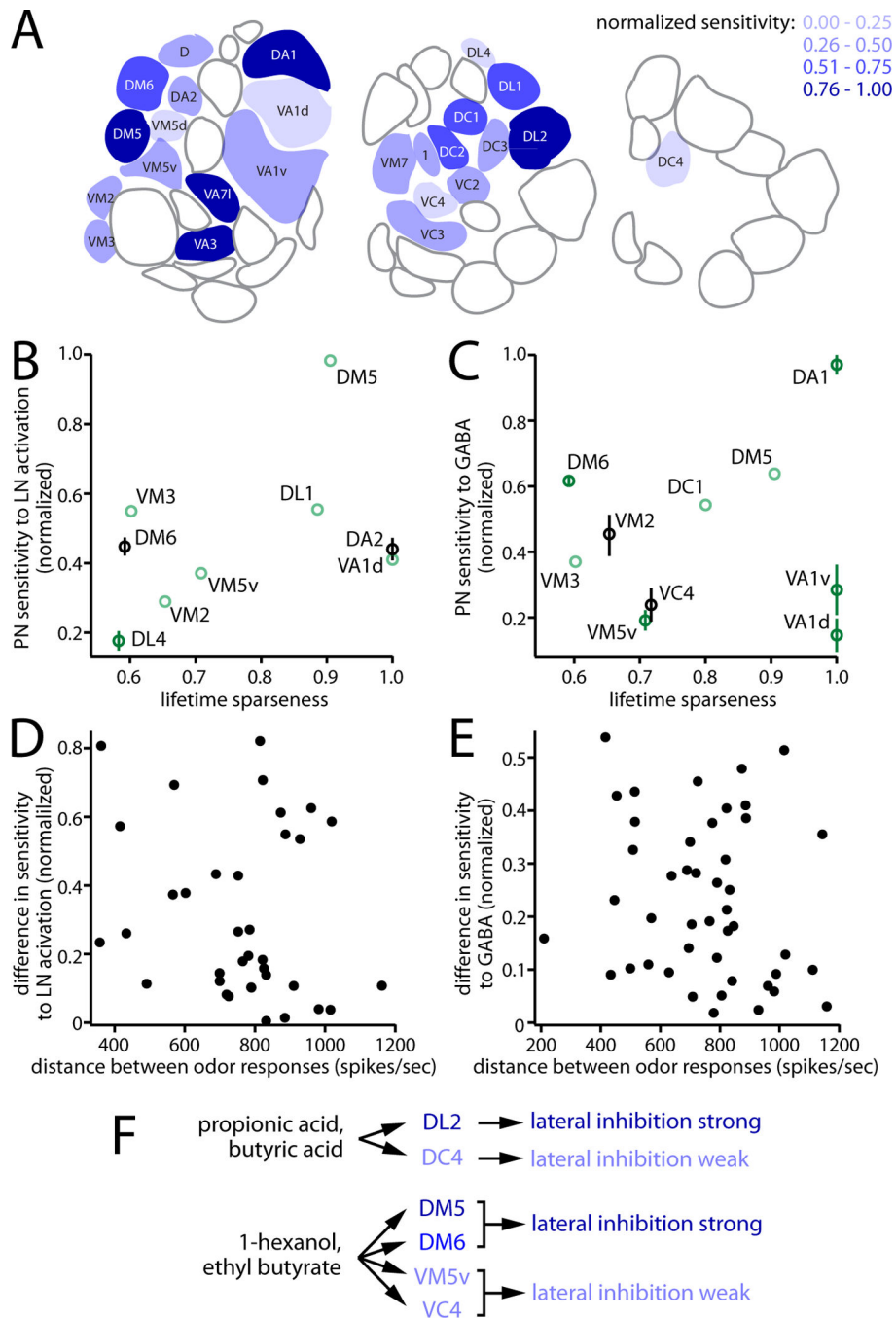
Figure 9. Sensitivity to inhibition is orthogonal to odor tuning

(A) Schematic showing three sections through the antennal lobe, from anterior (left) to posterior (right). Glomeruli are color coded according to their sensitivity to LN activation and/or GABA, with dark blue being the most sensitive and light blue the least sensitive. White glomeruli were not sampled.

(B) For each glomerulus, sensitivity to LN activation is plotted against the odor selectivity of its cognate odorant receptor, quantified as lifetime sparseness (0, nonselective; 1, maximally selective). There is no significant correlation (R^2=0.17, p=0.27). Light green points are

singly sampled; dark green points are sampled 2 – 4 times; black points are sampled at least 5 times. All p-values were determined by a permutation analysis (see Supplemental Experimental Procedures).

(C) Same as (B), but for sensitivity to GABA (R^2=0.02, p=0.71).

(D) Difference in sensitivity to LN activation versus the Euclidean distance between ORN response profiles, for every pairwise combination of sampled glomeruli (R^2=0.04, p=0.26).

(E) Same as (D), but for sensitivity to GABA (R^2=0.03, p=0.26).

(F) Odors are simultaneously encoded by glomeruli subject to strong lateral inhibition, and other glomeruli subject to weak lateral inhibition.